Water-Rock Interactions, Ore Deposits, and Environmental Geochemistry: A Tribute to David A. Crerar
© The Geochemical Society, Special Publication No. 7, 2002
Editors: Roland Hellmann and Scott A. Wood

In situ speciation of uranium(VI) at the silica-water interface: A combined TRLIFS and surface complexation study

UTA GABRIEL[1]*, LAURENT CHARLET[1], AND CARL W. SCHLÄPFER[2]

[1]Laboratoire de Géophysique Interne et Tectonophysique, OSUG, UJF - CNRS (UMR 5559)
Grenoble, France
[2]Institut de Chimie Inorganique, Université de Fribourg, Switzerland
*Corresponding author, present address: INRS Géoressources, Université du Québec,
C.P. 7500, Sainte-Foy, QC, G1V 2L2, Canada (e-mail: ugabriel@NRCan.gc.ca)

Abstract—The sorption of uranyl ions ($U^{VI}O_2^{2+}$) to amorphous silica has been studied by laser-induced time-resolved fluorescence spectroscopy (TRLIFS) at trace concentration levels (1 and 0.1 μM) in the presence of atmospheric CO_2. Uranyl is adsorbed on silica between pH 4 and 8.8, and two uranyl surface complexes have been identified in this pH range by their fluorescence properties. Characterized by distinct lifetimes (170 ± 25 μs at low pH and 360 ± 50 μs at high pH) and luminescence emission spectra (250 cm^{-1} red shift between the low pH and high pH spectra), they have been assigned to the $\equiv SiO_2UO_2^\circ$ and $\equiv SiO_2UO_2OH^-$ species. When fluorescence data were compared to analytically determined total sorbed concentrations, a third non-luminescent ternary surface complex ($\equiv SiO_2UO_2OHCO_3^{3-}$) had to be postulated to account for adsorption between pH 8.0 and 8.8.

The ability of uranium-rich silica particles to aggregate, and thus not to migrate in soils, was assessed by a series of centrifugation experiments using silica suspensions at pH 4.4 and 8.4. About 20 % of the total uranyl concentration (U_{tot} = 1 μM) is easily removed by centrifugation (1000 rpm, 5 minutes) and can considered to be immobile, as these particles aggregate easily in natural porous media. Under more rigorous centrifugation conditions (10,000 rpm, 40 to 60 minutes) the intermediate mobility fraction is removed. The uranyl removal is 98 % at pH 8.4, but only 70 % at pH 4.4. Of the 30 % of U_{tot} that is mobile at pH 4.4, 17 % fluoresces, and of this amount, 7 and 10 % are assigned to the sorbed and the dissolved uranyl fractions, respectively. Therefore, the risk of silica particle-induced transport of uranyl is more elevated in slightly acidic waters.

1. INTRODUCTION

Silica comprises a major part of igneous and metamorphic rocks of the earth's continental crust, including minerals in sedimentary environments (sand, biogenic silica, etc.). Consequently, adsorption on silica affects many superficial processes such as weathering rates, scavenging of diverse elements in the ocean, and the fate of contaminants in soils and groundwaters (Van Cappellen and Gaillard, 1996; Van Cappellen and Qui, 1997). All of these phenomena are controlled by chemical processes taking place at the interface between the mineral surface and the bulk solution. During the past decade, considerable progress has been made in the study of silica surface chemistry (Giamelo et al., 1990; Costa et al., 1990; Belyak et al. 1993; Dove and Rimstidt, 1994), dissolution kinetics (Dove and Crerar, 1990; Brady and Walther, 1990), and sorption of certain aqueous ions (e.g., thorium: Östhols, 1995; uranyl: Michard et al., 1996). However, the identity and structure of the actual surface species controlling the processes on the silica/water interface remain subject to controversy.

Owing to the development of surface-sensitive spectroscopic techniques such as infra-red spectroscopy (IR), nuclear magnetic resonance spectroscopy (NMR), low-energy electron diffraction (LEED), atomic force microscopy (AFM), and X-ray absorption spectroscopy (XAS) (Burneau and Gallas, 1998; Hommel et al., 1998; Reich et al., 1998; Sylwester et al., 2000; Dent et al., 1992), direct atomic level information on bonding environments at the silica/water interface has become available.

Based on surface titration and electrokinetic measurements (Schindler et al., 1976; James and Healy, 1972), surface complexation models (SCM's) of silica minerals were developed which postulate the formation of inner-sphere $\equiv OMe^+$ and $\equiv OMeOH^\circ$ surface complexes between a metal cation (Me^{2+}) and a primary surface hydroxyl $\equiv OH^\circ$ site (e.g. a surface silanol group). The various applications of these models for the interpretation of adsorption data and reaction kinetics demonstrated their validity in describing the speciation at the mineral/water interface. In the presence of CO_2 and an excess of metal ions with respect to surface reactive sites, the following species are assumed to form: $\equiv OMe^+$, $\equiv OMeOH^\circ$, $\equiv OMe(HCO_3)^{2-}$, and $\equiv OMe(OH)_2^\circ$. These surface species have been

inferred indirectly from surface titration, electrokinetics, adsorption, and reactive transport data, and from an analogy between the formation of surface and aqueous species (Schindler, 1991).

The present study focuses on the uranyl cation (UO_2^{2+}), which is used as a fluorescent molecular probe of the silica/water interface. Time-resolved laser-induced fluorescence spectroscopy (TRLIFS) allows an in situ investigation of the complexes it forms at the silicate surface. The uranyl ion is the most common and mobile form of uranium in oxidizing aqueous media. It is present in large concentrations in mining waste sites, atomic weaponry installations, and is expected in worst case scenarios to migrate out of spent nuclear fuel disposal sites and penetrate into soils and aquifers. Laser-induced fluorescence spectroscopy has long been a useful technique for characterizing the molecular environment of long fluorescence lifetime compounds (rare earth elements, uranyl ion, organic molecules) and their interactions with the surface of silica (Glinka and Krak, 1995; Kushnirenko et al., 1993; Stanton and Maatman, 1963; Wheeler and Thomas, 1984).

The main advantage of TRLIFS over the widely used XPS and EXAFS methods is that the former can provide detailed information on surface species present at very low surface concentrations. In addition, small changes (e.g., during hydrolysis) in the environment of the monitored molecular probe can be measured. This technique also has the advantage of not requiring any ultrahigh vacuum conditions. Since the laser beam interacts with the investigated suspension in a non-perturbing manner, the surface composition remains practically unchanged during the spectroscopic investigation.

In the present study we report on the first in situ spectroscopically-observed speciation of uranyl ions sorbed on amorphous silica. This TRLIFS-based speciation is compared with that obtained by standard macroscopic surface complexation models. We further study the centrifugation of U-rich particles at various pH's, centrifugation speeds, and centrifugation times. Based on these parameters, the risk of free uranyl and uranyl-silica particle transport is assessed.

2. METHODS

2.1. Experimental Methods

The silica sample used in this study (Aerosil 200) was provided by Degussa (Germany). It is a non-porous, X-ray amorphous material composed of spherical particles with a diameter of about 25 nm and a specific surface area of 169 m^2/g (Östhols, 1995). All chemicals used in this study were of p.a. grade.

Amorphous silica suspensions (particle concentration c_p = 1 g dm^{-3}) were prepared in 50-cm^3 polypropylene bottles in equilibrium with the atmosphere, at room temperature (22 ± 1 °C). For each of the three total uranyl concentrations (0, 0.1, and 1 μM) a series of 11 samples was prepared, with pH values adjusted between 3 and 9 using varying proportions of HNO_3 and Na_2CO_3 solutions at low and high pH values, respectively. $NaNO_3$ was added (mainly at low and intermediate pH values) in order to adjust the ionic strength to 0.01 M. The samples were shaken for at least one week at room temperature. Afterwards, the pH was measured once again and this final pH registered. A combination glass electrode (Metrohm) was calibrated using standard buffer solutions (Merck). Silica concentrations were determined colorimetrically using the molybdate blue method (Strickland and Parsons, 1972).

2.2. Time-resolved Laser-induced Fluorescence Spectroscopy (TRLIFS)

The fluorescence spectra for the surface speciation analysis were recorded at the Radiochemistry Institute, Research Center Rossendorf, Germany, using the following instruments and devices. The suspension samples were introduced into a fluorescence measurement cell (quartz, 4 cm^3, path length 1 cm; stirred) and excited with a pulsed NdYAG laser at 266 nm (Spectra Physics, 4 mJ/pulse, 8 ns pulse duration). The fluorescence was captured with an optic fiber (length: 0.5 m; Spectrophysics). The spectra were registered using a diode array (EG&E, 700 diodes, 0.3 nm resolution). The diode array was controlled by a delay generator (600 V) which was triggered by the laser itself and delayed by a delay generator. The energy delivered by the laser was controlled by an optical meter after passing the measurement cell. Previously, this experimental set-up was used to characterize the fluorescence of the uranyl ion in 0.1 M $HClO_4$. Bernhard et al. (1996) reported a lifetime of 1.55 ± 0.2 μs, which agrees with the values of 1.7 ± 0.2 μs measured by Eliet at al. (1995) and 1.9 ± 0.2 μs by Kato et al. (1994).

The experimental conditions of the present measurements are listed in Table 1. The delayed time gate (40.1 μs) was chosen in order to eliminate the fluorescence of dissolved uranyl hydroxyl, nitrate, and carbonate complexes (speciation in Fig. 1, equilibrium constants in Table 2) which are known to have lifetimes of about 33 μs or less (Eliet et al., 1995; Deniau et al., 1993). Uranyl sorbed on silica is known to have elevated lifetimes (Wheeler and Thomas, 1984: 440 μs). Duff et al. (2000) also reported elevated luminescence lifetimes for uranyl sorbed on lake

Table 1. Measurement conditions for the characterization of the surface complexes

delay	40.1 µs
gate	10 µs
delay step	5 and 2 µs
number of time steps	31
laser shots per spectrum	200
spectra per measurement	3

sediments (lifetimes ≤ 526 µs, measured at liquid N_2 temperature). The fluorescence of the dissolved uranyl silicic acid complex ($UO_2H_3SiO_4^+$) is thought to depend on silicic acid polymerization (Moll et al., 1998). Uranyl luminescence lifetimes of 19 ± 4 µs and 90 to 200 µs are reported in the presence of monomeric and polymeric silicic acid, respectively. Therefore, the dissolved uranyl silicic acid complex has to be considered in the fluorescence data interpretation. The silicic acid concentration in the present study was measured and found to vary from 1.5 to 2.2 mM, depending on pH. Speciation of uranyl ion in the presence of 2 mM silicic acid is given in Fig. 1.

In order to characterize uranyl surface complexes by their emitted time-resolved fluorescence spectra, one must first deconvolute all other fluorescence components. The fluorescence of solution complexes was already discussed. The silica suspension without uranyl (due to possible impurities of the silica or to defects in the lattice of the silica particles) also emitted a fluorescence signal in the studied wave number range. The spectra depict a broad, symmetrical, and rather noisy maximum at about 20,000 cm^{-1} (Fig. 2). The luminescence intensity could be described with a bi-exponential decay function (lifetimes of 8 ± 1 and 53 ± 4 µs). Neither the peak positions in the spectrum nor the lifetimes changed as function of pH (3 ≤ pH ≤ 8). This fluorescence signal should be present in all samples and independent of the uranyl adsorption. This spectrum was therefore subtracted from all of the spectra of the uranyl-silica system, thereby resulting in a zero baseline outside the range of the characteristic peaks of the uranyl fluorescence (for details see Gabriel, 1998). Typical spectra of the water-amorphous silica-uranyl system at a total uranyl concentration of 1 µM are given in Fig. 3.

The removal of particles from solution was assessed by a series of centrifugation experiments, in which both centrifugation time and speed were varied. Two 200-ml samples (pH 4.4 and 8.4) were prepared. After centrifugation (Beckmann Avanti J-20 centrifuge, fixed angle rotor JA-14, polypropylene tubes 40 ml), the fluorescence decay of the original and the supernatant solutions were recorded in the 50- to 450-µs time range using a pulsed nitrogen laser (VSL-337ND, Laser Science, Inc.; 250 µJ/pulse, 15 Hz, wave length 337 nm), a fluorescence measurement cell (quartz, 4 cm^3, path length 1 cm, stirred), a photomultiplier (Hamamatsu 94302, 500 V), a gelatin filter (Kodak 55, maximal transmission 67-69 % at 510-520 nm), a digital oscilloscope (digitizing oscilloscope

Table 2. Equilibrium constants (log K) for solution speciation (Grenthe et al., 1992; Stumm and Morgan, 1996, Moll et al., 1998)

Reaction			**log K (I=0)**	**log K (I=0.01)**
$UO_2^{2+} + H_2O$	↔	$UO_2OH^+ + H^+$	-5.2	-5.3
$UO_2^{2+} + 2\ H_2O$	↔	$UO_2(OH)_2^\circ + 2\ H^+$	-10.3	-10.4
$UO_2^{2+} + 3\ H_2O$	↔	$UO_2(OH)_3^- + 3\ H^+$	-19.2	-19.2
$UO_2^{2+} + H_2CO_3^\circ$	↔	$UO_2CO_3^\circ + 2\ H^+$	-7.0	-7.1
$UO_2^{2+} + 2\ H_2CO_3^\circ$	↔	$UO_2(CO_3)_2^{2-} + 4\ H^+$	-16.4	-16.3
$UO_2^{2+} + 3\ H_2CO_3^\circ$	↔	$UO_2(CO_3)_3^{4-} + 6\ H^+$	-28.5	-27.7
$2\ UO_2^{2+} + 3\ H_2CO_3^\circ$	↔	$UO_2CO_3(OH)_3^{3-} + 5\ H^+$	-17.6	-17.7
$UO_2^{2+} + H_4SiO_4^\circ$	↔	$UO_2H_3SiO_4^+ + H^+$	-1.7	-1.8
$UO_2^{2+} + NO_3^-$	↔	$UO_2NO_3^+$	0.3	0.06
H_2O	↔	$OH^- + H^+$	-14.0	-13.9
$H_4SiO_4^\circ$	↔	$H_3SiO_4^- + H^+$	-10.0	-9.9
$H_4SiO_4^\circ$	↔	$H_2SiO_4^{2-} + 2\ H^+$	-23.0	-22.7
$H_2CO_3^\circ$	↔	$HCO_3^- + H^+$	-6.4	-6.3
$H_2CO_3^\circ$	↔	$CO_3^{2-} + 2\ H^+$	-16.7	-16.4

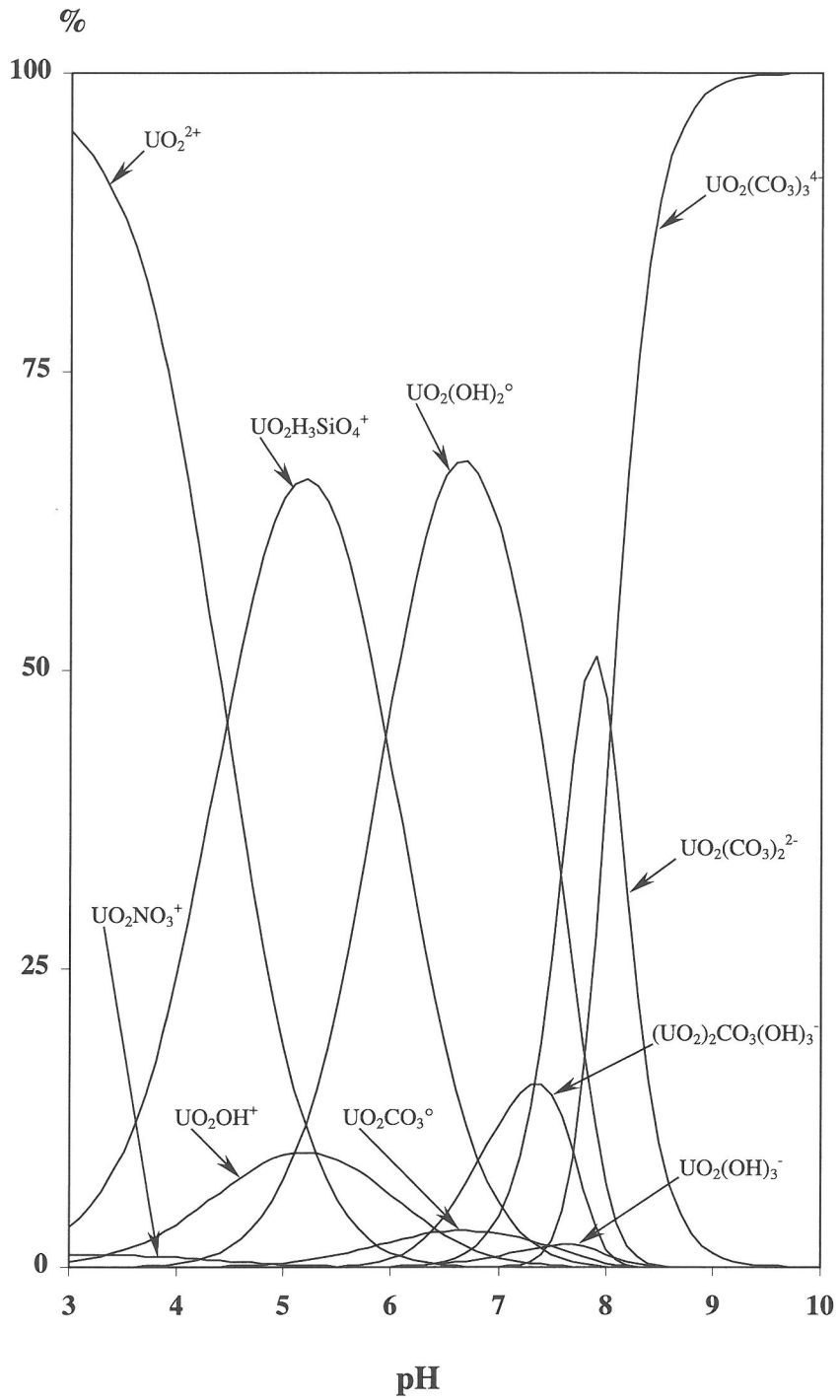

Fig. 1. Uranyl solution speciation based on the constants listed in Table 2 (Grenthe et al., 1992); code: GRFIT, Ludwig (1993); $[UO_2^{2+}]_{tot}$ = 1 μM; $[H_2CO_3°]_{free}$ = 22.4 μM; $[H_4SiO_4°]_{tot}$ = 2 mM; I = 0.01 M; $[NO_3^-]_{tot}$ = 0.01 M.

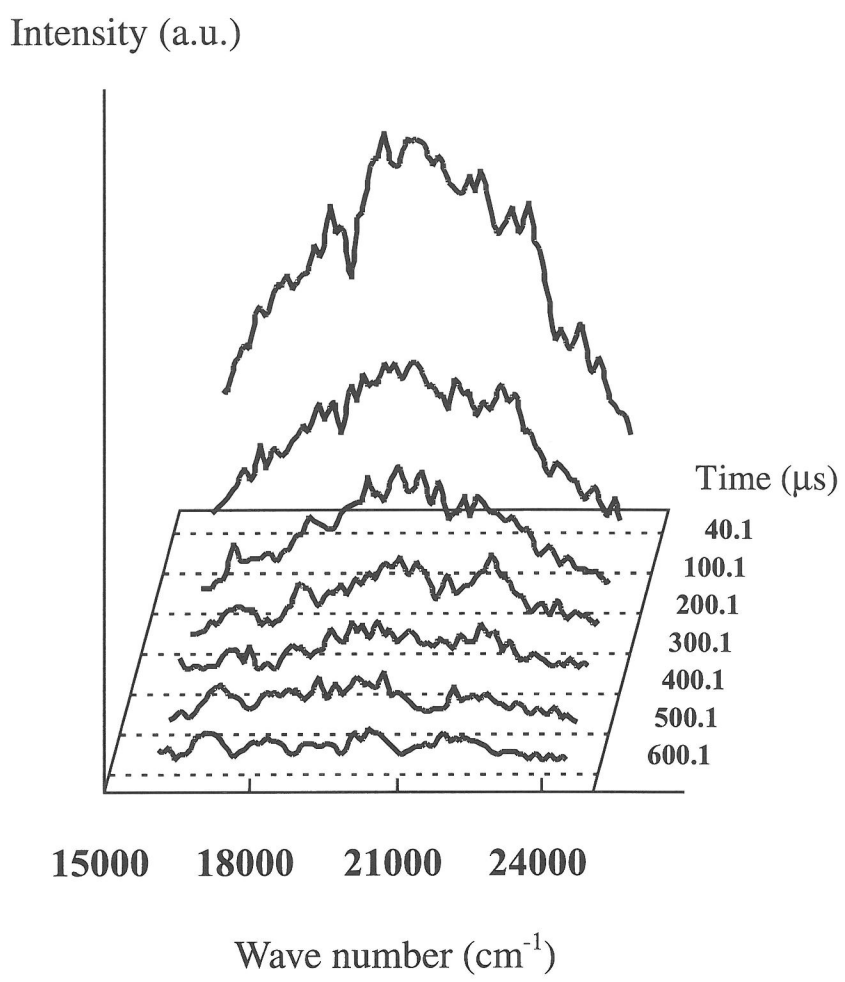

Fig. 2. Time-resolved luminescence spectra of a silica suspension at pH 5.11 (c_p = 1 g dm^{-3}; no uranyl ions).

54501A 100MHz, Hewlett Packard), and a photodiode (PIN S1223-01, Hamamatsu) at the Physical Spectrometry Laboratory, Grenoble, France. The fluorescence intensity is expressed in terms of % of the original suspension fluorescence (before centrifugation).

The sorption isotherms were measured by TRLIFS according to a third method, using the experimental set-up for fluorescence measurements at the Physical Spectrometry Laboratory, Grenoble, France. The suspensions were filtered through 0.45-μm filter membranes. No significant differences, with respect to dissolved uranyl concentrations, were observed when suspensions were filtered through 0.45-, 0.2-, 0.1-, and 0.025-μm filters. After filtration samples were instantly acidified to pH 1 with nitric acid to avoid sorption on the container walls. The dissolved uranyl concentration was measured according to the method given in Brina and Miller (1992). The addition of H_3PO_4 (final concentration 0.75 M) was used to form stable uranyl solution complexes with a typically long fluorescence lifetime of about 200 μs. This value is in good agreement with measurements of 200 μs by Moulin et al. (1995) and 232.1 ± 0.5 μs by Kato et al. (1994) and Meinrath et al. (1993).

The initial fluorescence intensity is proportional to the concentration of the emitting molecules. By extrapolation of the exponential decay to time zero, the initial fluorescence intensity was determined. The method was calibrated using the standard additions method. Corrections were made for base line and

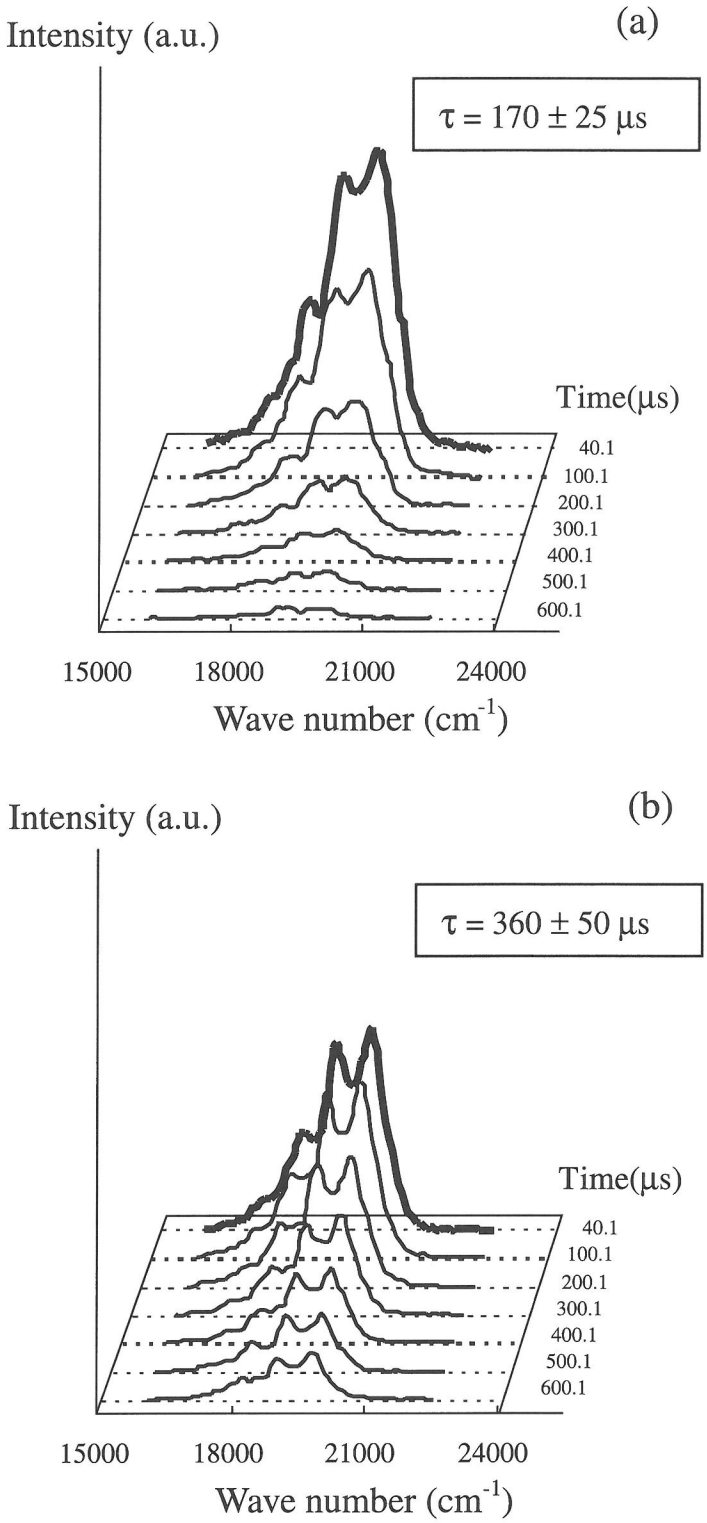

Fig. 3. Experimental time-resolved luminescence spectra of silica suspensions at pH 4.4 (a) and pH 8.2 (b). Intensities are shown in the same arbitrary units; $[UO_2^{2+}]_{total}$ = 1 μM; c_p = 1 g dm^{-3}. The spectra obtained 40.1 μs after the laser pulse (thick lines) have been used in Figs. 4 and 5.

instrumental drift. The detection limit and precision were 3 nM and 5 %, respectively (Gabriel et al., 1998).

2.3. Data Treatment

The fluorescence emitted by complex i is a function of the time t and wave number ν, and its decay follows an apparent first order law (Brina and Miller, 1992):

$$I_i(t,\nu) = I_i(0,\nu)\exp\left(-\frac{t}{\tau_i}\right) \quad (1)$$

where $I_i(t,\nu)$ is the fluorescence intensity of complex i at the wave number ν and time t; τ_i is the characteristic fluorescence lifetime of complex i.

When all parameters of the experiment are kept constant, the observed fluorescence intensity $I_i(t,\nu)$ of species i at time t and wave number ν is related to the concentration S_i of the emitting complex i by:

$$I_i(t,\nu) = \omega_i(t,\nu)\, S_i \quad (2)$$

where $\omega_i(t,\nu)$ is an experimental parameter. It incorporates the effects of absorption, radiant and non-radiant transition probabilities (all characteristic for the emitting complex i), and several parameters characteristic of the experimental set-up, such as pre-filter and post-filter effects. A detailed discussion of this is given by Berthoud et al. (1988) and Eliet (1996). The vector $\omega_i(t,\nu{=}1\ ..\ l)$ represents the fluorescence spectrum of species i (l is the number of data points in the spectrum).

The fluorescence intensity of n emitting complexes is additive. The overall fluorescence intensity of a composite solution or suspension is then described by

$$I_i(t,\nu) = \sum_{i=1}^{n} \omega_i(t,\nu)\, S_i \quad (3)$$

The sum of concentrations of all emitting surface complexes, S_i, is equal to or smaller than the analytically-determined total concentration of sorbed uranyl ion, S_{tot}:

$$S_{tot} \geq \sum_{i=1}^{n} S_i \quad (4)$$

The difference between S_{tot} and the summation on the right-hand side (Eqn. 4) gives the concentration of possible silent, non-emitting surface species. Concentrations of all emitting complexes are related to the emitted fluorescence light, given by Eqn. 3. Two parameters, $\omega_i(t,\nu)$, the emission at a given time t and a wave number ν, and the emission lifetime τ_i , are characteristic of an adsorbed species. These parameters were used separately in order to obtain quantitative information with respect to the surface speciation.

2.3.1. Wave number-resolved data (spectra at 40.1 μs)

In order to reduce the data from the spectra from 700 to 60 we smoothed the experimental data using the built-in function of the software package Mathcad 6+ (spline).

At a given time t the measured fluorescence intensity $I(\nu)$, given by:

$$I(\nu) = \sum_{i=1}^{n} \omega_i^t(\nu)\, S_i \quad (5)$$

is analogous to the Lambert-Beer law for absorption. The fluorescence of a series of suspensions is given by the following matrix equation (dimensions of the matrices are given in brackets)

$$\mathrm{I}(l,s) = \mathrm{w}(l,n)\ \mathrm{S}(n,s) \quad (6)$$

with

- $I(l,s)$ matrix of the measured fluorescence intensities. The columns are the emission spectra for the given solution.
- $w(l,n)$ matrix of the fluorescence spectra. The columns give the emission spectra of the significantly different surface complexes.
- $S(n,s)$ matrix of the relative concentrations. The columns give the speciation of the surface species.
- l number of data points per spectrum
- s number of solutions (or measured spectra)
- n number of significantly different complexes

The mathematical procedure consists of decomposing the matrix of the fluorescence data $I(l,s)$ into a linear product of the matrices of the relative concentrations of the fluorescent complexes $S(n,s)$ and their specific fluorescence spectra $w(l,n)$.

Singular value decomposition of $I(l,s)$ allows for the determination of the number of emitting species n. Evolving Factor Analysis (EFA, Gampp et al., 1987) can be used for the model-free decomposition of the matrix $I(l,s)$ after the number of species have been determined, based on the following conditions:

1. linear relationship between the measured fluorescence intensity at time t and the concentration of the fluorescent complex S_i (Eqn. 2)
2. mass conservation
3. the first and the last spectrum are due to only one species, respectively
4. when stepping from one pH to another only one new emitting species appears
5. the species disappear as pH increases in the same order as they appeared (i.e., "first in - first out").

The condition of the mass conservation is easily replaced by Eqn. 4 if linear programming (Press et al., 1992) is used to solve the optimization problem.

2.3.2. *Time-resolved integral values of the fluorescence intensity (decays)*

The EFA of the spectra indicated that two complexes dominate the experimental fluorescence spectra of the suspensions containing 1 µM uranyl. Thus, Eqn. 3 can be reduced to a two-term equation. At a given wave number ν (or within a given ν range) the experimental decay is described by:

$$I(t) = \omega_1^0 S_1 \exp\left(-\frac{t}{\tau_1}\right) + \omega_2^0 S_2 \exp\left(-\frac{t}{\tau_2}\right) \quad (7)$$

The experimental intensity integral $I(t)$ between 19000 and 20000 cm^{-1} was used.

2.4. *Surface Complexation Modeling*

The adsorption chemical equilibrium of uranyl ions onto silica by surface complexation can be described by the general equation:

$$p \equiv Si(OH)_2 + q\, UO_2^{2+} + r\, H^+ + s\, CO_3^{2-} \leftrightarrow \left(\equiv Si(OH)_2\right)_p \left(UO_2\right)_q (H)_r \left(CO_3\right)_s^{(2q+r-2s)} \quad \beta^s_{pqrs} \quad (8)$$

where β^s_{pqrs} is the conditional equilibrium constant, and p, q, r and s are the (positive or negative) stoichiometry coefficients. The conditional equilibrium constant includes activity coefficients for solution species which were calculated with the Davies equation (Davies, 1962). Activity coefficients for all surface species are assumed to be equal to 1. The $\equiv Si(OH)_2$ surface species is a hypothetical average surface adsorption site, susceptible to lose one proton according to:

$$\equiv Si(OH)_2 \rightarrow \equiv SiO_2H^- + H^+ \qquad \beta^s_{10-10} \quad (9)$$

The total concentration of surface sites $[\equiv Si(OH)_2]_{tot}$ was set to 0.51 mM (after Östhols, 1995) and the total uranyl ion concentration $[UO_2^{2+}]_{tot}$ was defined as constant. The total proton concentration $[H^+]_{tot}$ is calculated using a charge-balance expression. The free carbonic acid concentration $[H_2CO_3]_{free}$ is controlled by CO_2-equilibrium with the atmosphere ($P_{CO_2} = 10^{-3.51}$ atm).

The conditional equilibrium constants β_{pqrs} and $\beta_{10\text{-}10}$ were corrected for the Coulombic energy of the surface charge to obtain the corresponding intrinsic constants:

$$\beta^s_{pqrs(\text{int})} = \beta^s_{pqrs} \exp\left(\frac{(2q+r-2s)F\Psi}{RT}\right) \quad (10)$$

where Ψ is the effective surface potential. The total molar charge of the surface σ_{tot} is given by:

$$\sigma_{tot} = \sum_p \sum_q \sum_r \sum_s (2q+r-2s)\beta^s_{pqrs} \times \left[\equiv Si(OH)_2\right]^p \left[UO_2^{2+}\right]^q \left[H^+\right]^r \left[CO_3^{2-}\right]^s \quad (11)$$

To relate the total molar surface charge σ_{tot} to the surface potential Ψ the constant-capacitance model (Schindler and Gamsjäger, 1972) was used, since the formation of outer-sphere complexes could be excluded (Dent et al., 1992; Reich et al., 1996; 1998; Sylwester et al., 2000):

$$\Psi = \frac{\sigma_{tot} F}{A_s c_p \kappa} \quad (12)$$

where A_s is the specific surface area ($m^2\ g^{-1}$), c_p is the particle concentration ($g\ dm^{-3}$), F is the Faraday constant, and κ is the capacitance ($F\ m^{-2}$). The intrinsic stability constants, the total site concentration, and the capacitance were determined from the adjustment of the experimental fluorescence data using the program GRFIT (Ludwig, 1993). The evaluation was based mainly on the goodness-of-fit (Westall, 1982).

3. RESULTS AND DISCUSSION

3.1. *Identification of Different Surface Complexes*

In Fig. 4 the experimental uranium fluorescence spectra recorded on silica suspensions equilibrated at different pH values and total uranyl concentrations (1 and 0.1 µM) are compared. The spectra recorded for different total uranium concentrations reveal similar behavior. At pH values below 4.4 the fluorescence signal is very weak, but around pH 4.4 the intensity increases strongly. In this pH range (pH ≤ 4.4), macroscopic sorption measurements indicate that the concentration of sorbed uranium shifts from 50 % to 80 % of the total uranyl concentration (discussed further on). The fluorescence spectra in this pH range show the same maximum peaks, whatever the total uranium concentration, and the same uranyl molecular environment is assumed to dominate the fluorescence signal. In the 4.5 to 5.5 pH range the fluorescence intensity remains at the same elevated level, but a second component appears in the spectra, which is characterized by maxima at smaller wave numbers (i.e. with a 250-cm^{-1} red shift). In the pH range 5.5 to 8 the spectra are dominated by this sec-

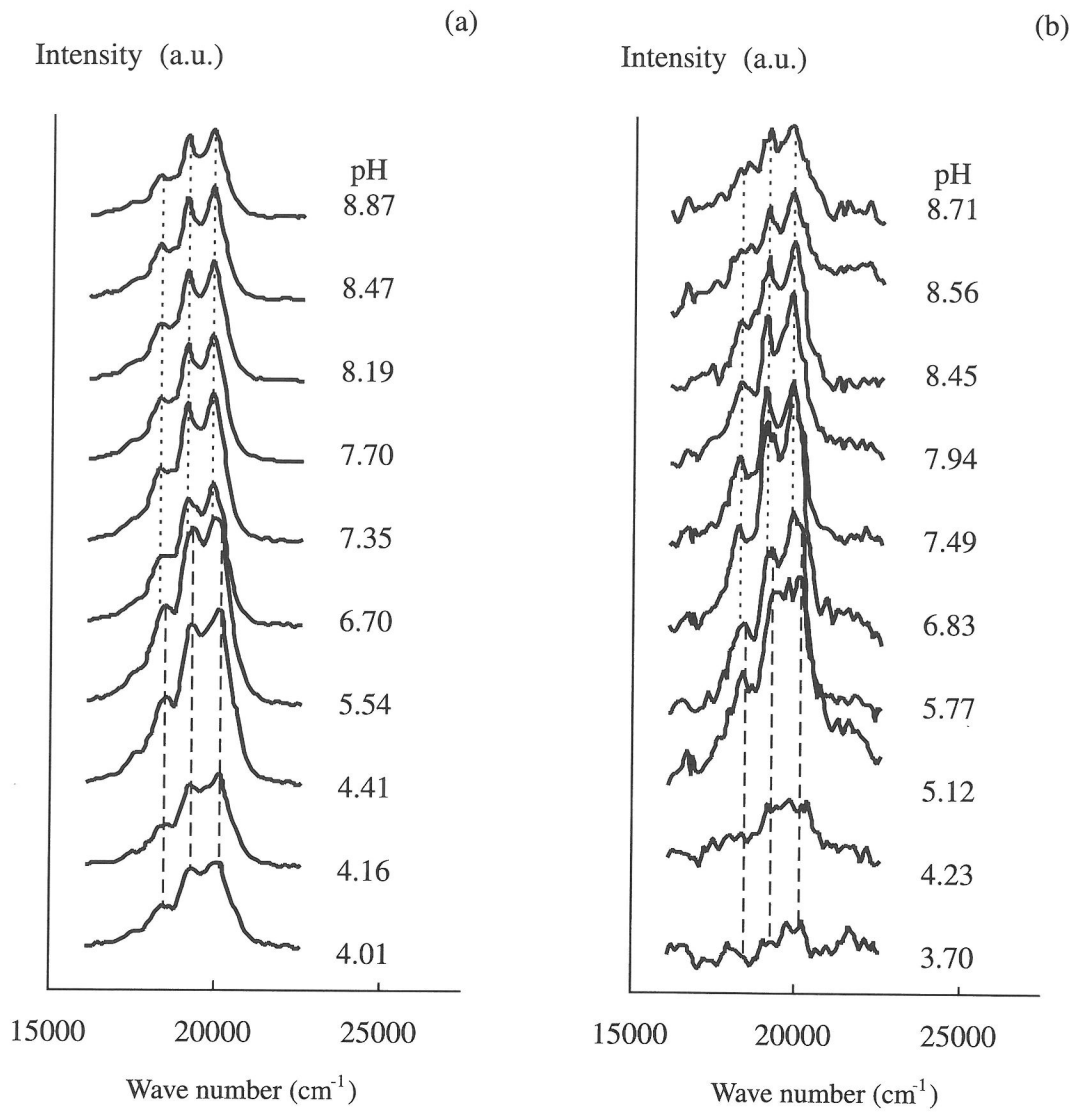

Fig. 4. Experimental spectra of the silica suspensions (c_p = 1 g cm^{-3}) containing 1 μM (a) and 0.1 μM (b) uranyl; intensity values are divided by 10 for (a).

ond component spectrum. Beyond pH 8.2, the overall intensity decreases.

A comparison of both fluorescence components indicates that they also differ as a function of their lifetimes. A longer lifetime is observed for the higher pH fluorescence component (Fig. 3). By an adjustment of a mono-exponential decay function to the experimental data, lifetimes of 170 ± 25 and 360 ± 50 μs were determined for samples prepared at low and high pH values, respectively. The mono-exponential decays at pH 4.4 and 8.2 did not completely exclude the existence of minor fluorescence components at these pH values, but indicated nonetheless the dominance of distinct molecular environments in both spectra.

3.2. *Quantification of the Surface Speciation*

The spectra obtained for a total uranyl concentration of 1 μM (Fig. 4a) were analyzed by singular value decomposition (Gampp et al., 1987). This

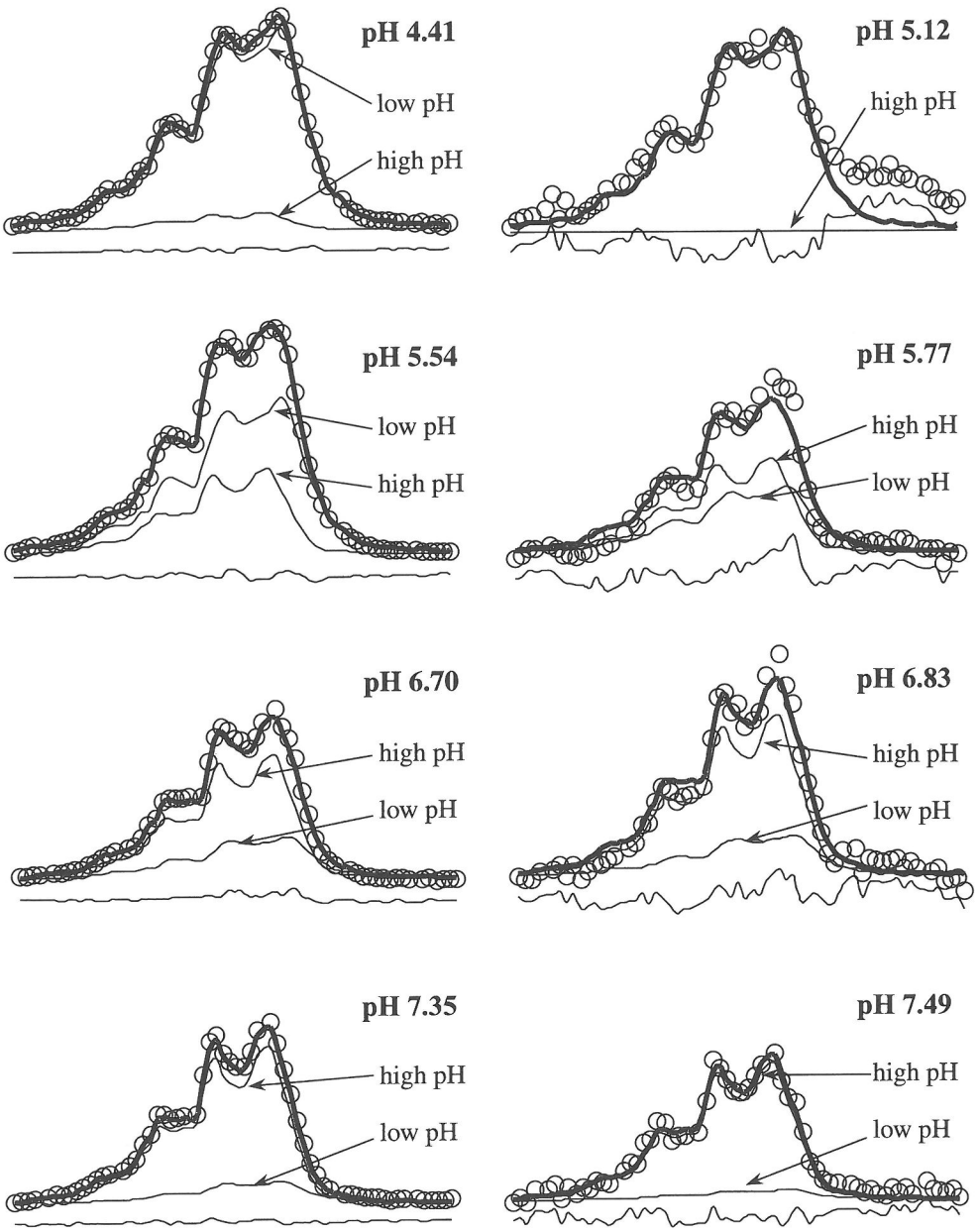

Fig. 5. Experimental spectra (o symbol) at a total uranyl concentration of 1 μM (left column) and 0.1 μM (right column), adjusted using evolving factor analysis (thin lines: prevailing spectra at low/high pH; thick line: sum of both; thin line below: remaining error; c_p = 1 g dm^{-3}; intensity values are divided by 10 for the left column).

analysis confirmed the existence of two distinctively different spectra. For the deconvolution of these spectra the evolving factor analysis (EFA) was used. The spectra of the intermediate pH values, where dominance shifts from the first spectrum to the second, are represented in the left column of Fig. 5. The already mentioned dominance shift between pH 5.5 and 6.7 is confirmed. The experimental data at a total uranyl

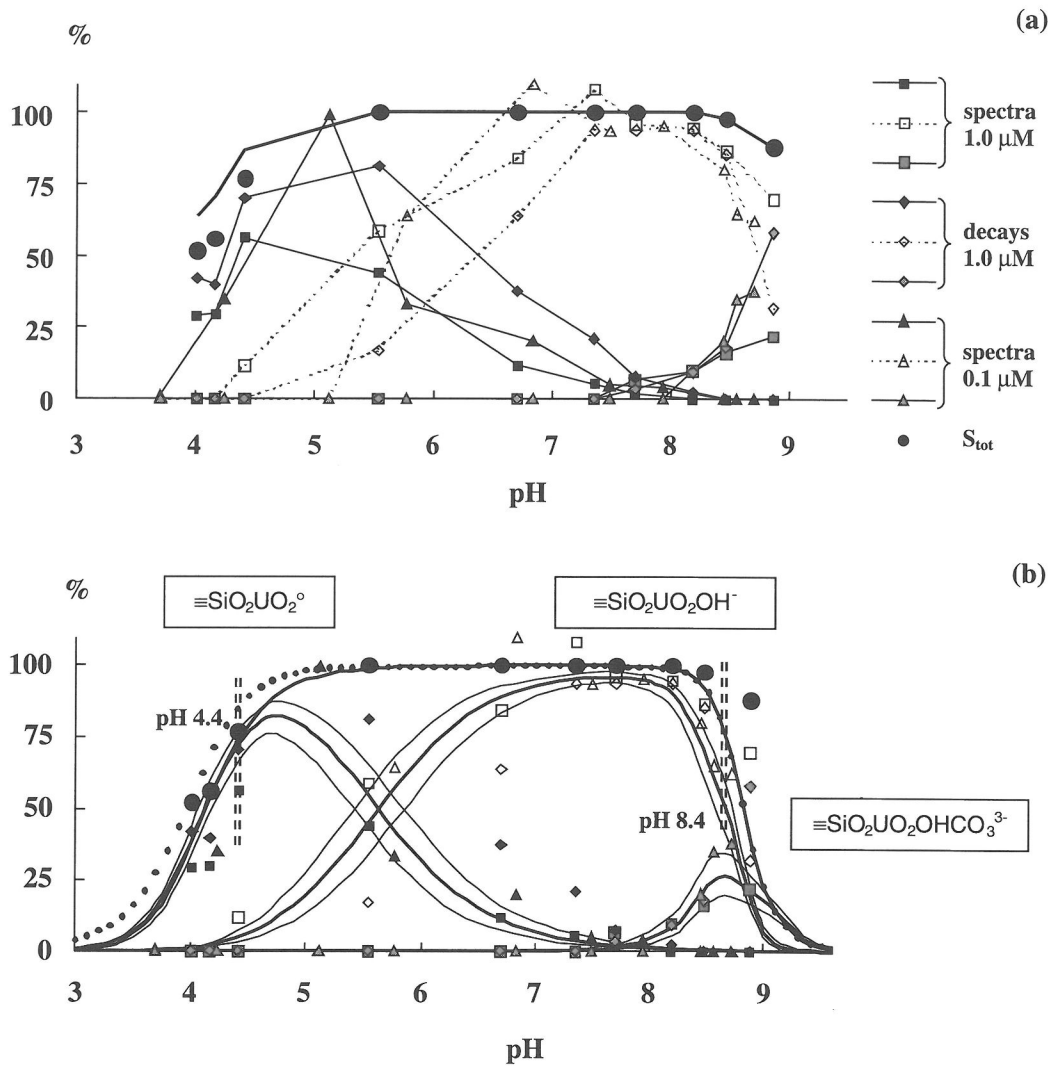

Fig. 6. Results of the experimental spectra and decays (a) and uranyl surface speciation model (b). Stability and intrinsic surface constants are given in Tables 2 and 3; filled and open symbols indicate the lower and higher protonated state; grey symbols show the silent surface complex contribution, i.e., the difference between S_{tot}, the sorbed amount of uranyl (filled circles, in % of total concentration) and the two luminescent surface complexes; thin lines in (b) show the sensitivity analysis; the thick line in (a) and small dots in (b) include the dissolved uranyl silicic acid complex (see text for details.)

concentration of 0.1 µM were adjusted with the same two composite spectra (right column in Fig. 5). The spectrum at pH 5.1 is still completely controlled by the first component spectrum, whereas at pH 5.8 both spectra have about the same importance. At pH 6.8 the second component dominates the spectrum.

In order to be able to deduce surface species from the intensities of the two fluorescence components, the overall sorbed concentration needed to be characterized. Uranyl ions are nearly completely removed from solution between pH 5.5 and 8.5 by adsorption on filterable silica (> 0.45 µm, large dots in Fig. 6). Below pH 4.4, two processes prevent uranyl adsorption: (i) protons compete efficiently with uranyl ions for silanol reactive groups and (ii) dissolved silicic acid, and very marginally also nitrate and hydroxyl ions, complex uranyl in solution (Fig. 1). On the other hand, above pH 8.5 dis-

solved carbonate ions out-compete surface silanol ligands for uranyl complexation. Stable $UO_2(CO_3)_3^{4-}$ are formed in solution, and uranyl adsorption starts declining (i.e., Fig. 1).

Since the uranyl complexed by (polymeric) dissolved silicic acid also emits a fluorescence signal with a long lifetime (90-200 µs, Moll et al. 1998), the sum of the concentrations of the emitting species may be greater than the total sorbed concentration in the low pH range. In order to evaluate this effect the concentration of the calculated dissolved uranyl silicate ($UO_2H_3SiO_4^+$) was added to the total sorbed concentration (thickest solid line in Fig. 6a), this resulting in positive % changes of 9, 10, and 6 at pH values of 4.0, 4.2, and 4.4, respectively. The large domain of complete adsorption between pH 5.5 and 8.5 is not affected. For this reason it was justifiable to set the measured total concentration of sorbed uranyl, S_{tot}, larger or equal to the sum of the concentrations of all the present uranyl containing surface complexes according to Eqn. 4. The relative concentrations of the two fluorescent surface complexes obtained by EFA are indicated in Fig. 6a by the filled and open squares (1 µM uranyl) and filled and open triangles (0.1 µM), respectively. The second component dominates beyond pH 5.5 ± 0.2. It appeared that the fluorescence yield at time 40.1 µs after the laser shot of the low-pH surface complex was about double the one of the high-pH surface complex (Figs. 3, 4).

In order to test whether the dissolved uranyl silicic acid complex has a different fluorescence spectrum than the surface species, 4 samples were centrifuged at relatively low speed for 10 minutes. In Fig. 7, the fluorescence spectra are compared. No spectral differences can be observed between the original and the centrifuged samples, suggesting that the spectral data, in contrast to the lifetime data, cannot be used to distinguish between surface and solution (polymeric/monomeric) uranyl silica species.

The initial intensities of the exponential decay functions (adjusted to the experimental decays in the 40.1 to 600.1 µs time range, data not shown, Gabriel, 1998) were used as a third indication for the concentrations of the two fluorescence components (diamonds in Fig. 6). The shift from one surface complex to another occurred at a slightly higher pH (between pH 5.5 and 6.7). Thus, the spectra and lifetime values at 1 µM uranyl lead to the same in situ speciation of uranium as in the silica suspension. The experimental decay signals of the 0.1 µM uranyl series were not used for the speciation estimation since the signal after 200 µs had a too low signal/noise ratio. It was therefore not possible to adjust a bi-exponential decay function.

A difference between the experimentally determined sorbed concentration S_{tot} and the sum of the concentrations of the two fluorescent surface complexes S_1 and S_2 was observed between pH 8 and 9. This difference was interpreted as being due to the presence of a non-fluorescent surface complex (relative concentrations are represented by gray-filled symbols in Fig. 6).

3.3. Surface Complexation Modeling

Uranyl adsorption on amorphous silica has been studied extensively by EXAFS (Dent et al., 1992; Reich et al., 1998; Sylwester et al., 2000). Adsorption is reported to take place in the equatorial plane formed around the U^{VI} atom of the linear uranyl ($O=U^{2+}=O$) cation. Free uranyl in an acid, non-complexing aquatic environment is surrounded by five to six water molecules, these forming the equatorial plane of the uranyl cation. In all complexation or adsorption reactions some of these water molecules are replaced by negatively charged ions, such as nitrate, hydroxyl, or surface groups (inner-sphere complexes). This leads to an uneven charge distribution in the equatorial plane. In some cases this leads to a splitting of the equatorial shell because the nearest atoms are likely to be found at different distances. This was observed by Waite et al. (1994) on ferrihydrite. Farges et al. (1992) confirmed the splitting of the equatorial shell in solids by XRD.

The measured small U-Si distances suggest that uranyl forms bi-dentate surface complexes. Sylwester et al. (2000) determined an U-U closest neighbor distance suggesting the existence of polymers at pH 6.46 and a total uranyl concentration of 41.5 µM. Based on the solubility of soddyite (Moll et al., 1996; Moll, 1997) precipitation is likely at $[UO_2^{2+}]_{tot}$ = 41.5 µM, but may also depend on the reaction rate. At pH 3.14 and a total uranyl concentration of 9.79 mM, no molecular U-U near-order was detected (Sylwester et al., 2000). Reich et al. (1998) studied uranyl adsorption on silica at even higher total uranyl concentrations (≤ 0.05 M in the pH range 3.5 to 4.5) and did not detect uranyl surface polymers. Based on the available evidence it is not possible to completely exclude the existence of uranyl hydroxy-polymers at the silica/water interface. However, the similarities in the present spectral data obtained for total uranyl concentrations that vary over one order of magnitude indicate mononuclear uranyl adsorption (Figs. 4a,b,5).

In the characterization of uranyl solution speciation, TRLIFS has been widely used to distinguish different hydrolysis states and polymers (Eliet et al., 1995; Brendler et al., 1996; Bernhard et al., 1996; Moulin et al., 1995). Hydrolysis and polymerization

can be observed by TRLIFS because charge distribution and symmetry in the equatorial plane change. Equatorial and axial oxygen bounding distances are inversely related (Pauling principle: Pauling, 1929; Hudson et al. 1995), this causing the altered fluorescence signal.

Based on all of the above information we propose two fluorescent surface complexes, each with a mono-nuclear bidentate structure. The adsorption reaction takes place in the equatorial plane where two of the five (or six) water molecules of the free uranyl are replaced by silanol surface groups, this resulting in the release of two protons (Table 3). The water molecules of the free uranyl ion have not been included in Table 3. The low-pH complex is assumed to be a neutral uranyl complex $\equiv SiO_2UO_2^\circ$. The second fluorescent surface complex is thought to include an additional hydroxyl ion (i.e., in its formation three protons are released: $\equiv SiO_2UO_2OH^-$).

One explanation for the non-observed fluorescence of the postulated surface complex at high pH may be the presence of carbonate ions, this leading to a ternary surface site-uranyl-carbonate structure. Bargar et al. (1999, 2000) have observed ternary uranyl carbonate complexes on hematite. The for-

Table 3. Intrinsic constants (log K) for silica surface speciation (constant capacitance model; c_p = 1 g dm^{-3}; A_s = 169 m^2 g^{-1}; κ = 7 F m^{-2}; $[NO_3^-]_{tot}$ = 0.01 M, $[\equiv Si(OH)_2]_{tot}$ = 0.51 mM; $[H_2CO_3^\circ]_{free}$ = 22.4 μM; $[H_4SiO_4^\circ]_{tot}$ = 2 mM; $[UO_2^{2+}]_{tot}$ = 1 μM)

Reactions			logK (I=0)	logK (I=0.01 M)
$\equiv Si(OH)_2$	↔	$\equiv SiO_2H^- + H^+$	-6.98	-6.94
$\equiv Si(OH)_2 + UO_2^{2+}$	↔	$\equiv SiO_2UO_2^\circ + 2\ H^+$	-4.69	-4.78
$\equiv Si(OH)_2 + UO_2^{2+} + H_2O$	↔	$\equiv SiO_2UO_2OH^- + 3\ H^+$	-10.33	-10.37
$\equiv Si(OH)_2 + UO_2^{2+} + H_2CO_3^\circ + H_2O$	↔	$\equiv SiO_2UO_2OHCO_3^{3-} + 5\ H^+$	-22.02	-21.98

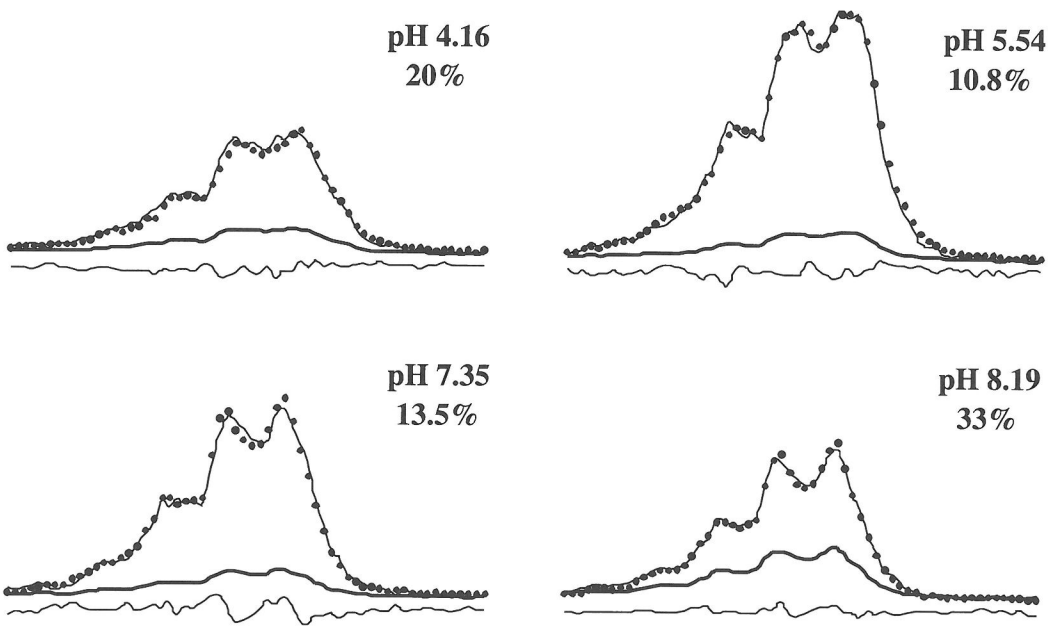

Fig. 7. Experimental spectra of the original (dots) and centrifuged suspensions (thick line). The adjusted thin line permits comparison of the magnified spectrum to the original one; the remaining error is represented by the thin lines below; percentages correspond to remaining fluorescence after centrifugation; total uranyl concentration = 1 μM.

mer study concluded that the entire pH range is dominated by ternary uranyl carbonate complexes. However, iron-bearing oxides and hydroxides are known to have a high affinity for dissolved carbonate, but this behavior is not known for silica surfaces.

Bernhard et al. (1996) reported uranyl complexation with carbonate in solution. This resulted in quenching of the fluorescence and therefore leading to no measurable signal 1 μs after the laser pulse. The same was found by Kato et al. (1994) who did not detect a fluorescence signal due to aqueous uranyl carbonate complexes. On the other hand, Bernhard et al. (1996) report fluorescence lifetimes of 270 and 300 μs for liebigite and zellerite (both uranyl carbonates), respectively. This might be due to a lesser amount of water in the molecular environment of uranyl in the mineralogical lattice.

For the non-fluorescent surface complex we propose the following structure: $\equiv SiO_2UO_2OHCO_3^{3-}$. Its formation involves the release of three protons. This complex has been included in the following surface speciation model, even though both its existence and structure are hypothetical for the moment. The surface speciation is represented by the thick lines in Fig. 6b. The optimum data fit was obtained with a capacitance κ of 7 F m^{-2}. This high capacitance value indicates a very thin double layer. The corresponding logarithmic complexation constants are summarized in Table 3. The logarithmic deprotonation constant of the silica surface was assumed to be 6.94, in accordance with the literature (Charlet et al., 1993; Östhols, 1995).

The most accurate region in the speciation diagram (Fig. 6b) is between pH 5.5 and pH 7. We evaluated the impact of a 0.1-log unit change in the equilibrium constants as a sensitivity analysis. The thin lines in Fig. 6b indicate the results showing (i) increases in the complexation constants (log K + 0.1) of the $\equiv SiO_2UO_2^{\circ}$ and $\equiv SiO_2UO_2OHCO_3^{3-}$ complexes and a decreased formation constant (log K – 0.1) of $\equiv SiO_2UO_2OH^-$, or (ii) the inverse. The sensitivity analysis showed that a 0.1-log unit change of the constants did not change the adsorption or the desorption edge, but shifted the intersection of the dominance fields of the first and second complexes from pH 5.5 to 5.9. The theoretical curves are closer to the experimental data deduced from the spectra than to those deduced from the luminescence decays. The differences between both data sets might be due to different sensitivities of the spectra and the luminescence decays with respect to certain structural parameters, such as bonding distances and symmetry.

3.4. Particle-facilitated Transport of Uranyl

Uranium sorbed on silica may be either mobile or immobile in the environment, depending on the particle mobility, i.e., depending on the tendency to aggregate in the subsoil. As was observed in preliminary experiments, centrifugation does not remove the entire fluorescence signal of the uranyl silica suspensions. This tendency was further studied in a series of centrifugation experiments performed on silica suspensions at equilibrium at two different pH values (4.4 and 8.4) with 1 μM uranium. Fluorescence decays (50 to 450 μs) of the supernatant were recorded after centrifugation at different times and velocities. Results are presented in Fig. 8, where the registered fluorescence intensity at 50 μs has been normalized to the intensity of the suspension before centrifugation (also at 50 μs).

Irrespective of the equilibrium pH (4.4 and 8.4), 20 % of the fluorescence is easily removed after a light centrifugation (5 minutes at 1000 rpm). At pH 4.4 (but not at pH 8.4) a further 45 % of the fluorescence is removed by centrifugation for 1 h at the same centrifugation speed. At pH 8.4 centrifugation at 1,000 rpm for one hour did not reduce the uranyl fluorescence in the supernatant. A high-gravity field (centrifugation at 10,000 rpm for 60 min) is needed to reduce the uranyl fluorescence to zero. However, at pH 4.4, even high-gravity fields (40 minutes at 10,000 rpm) were not able to remove more than another 15 % of the fluorescence signal, such that 20 % of the fluorescence signal remained in suspension and/or solution.

As already discussed in the quantification of the surface speciation, the fluorescence signal cannot simply be assumed to correspond directly to the total sorbed concentration because dissolved uranyl silica complexes potentially emit a similar luminescence signal. Therefore, at pH 4.4, the 20 % fluorescence signal which remains should be compared to the dissolved uranyl fraction which is complexed by silicic acid, which is 10 % of the total uranyl concentration. At this pH, 13 % of the total uranyl concentration is not bound to silicic acid and can therefore be assumed to have no long-life fluorescence. The sum of all the fluorescent fractions (sorbed and dissolved) can be assumed to correspond to 87 % of the total uranyl concentration. On this basis the different fractions at pH 4.4 (Fig. 9) have been calculated. The non-removable fluorescence fraction is attributed partly to the sorbed (7 %) and partly to the dissolved (10 %) uranyl. With respect to these interpretations, it must be kept in mind that experimental artifacts, such as the incomplete removal of silica particles

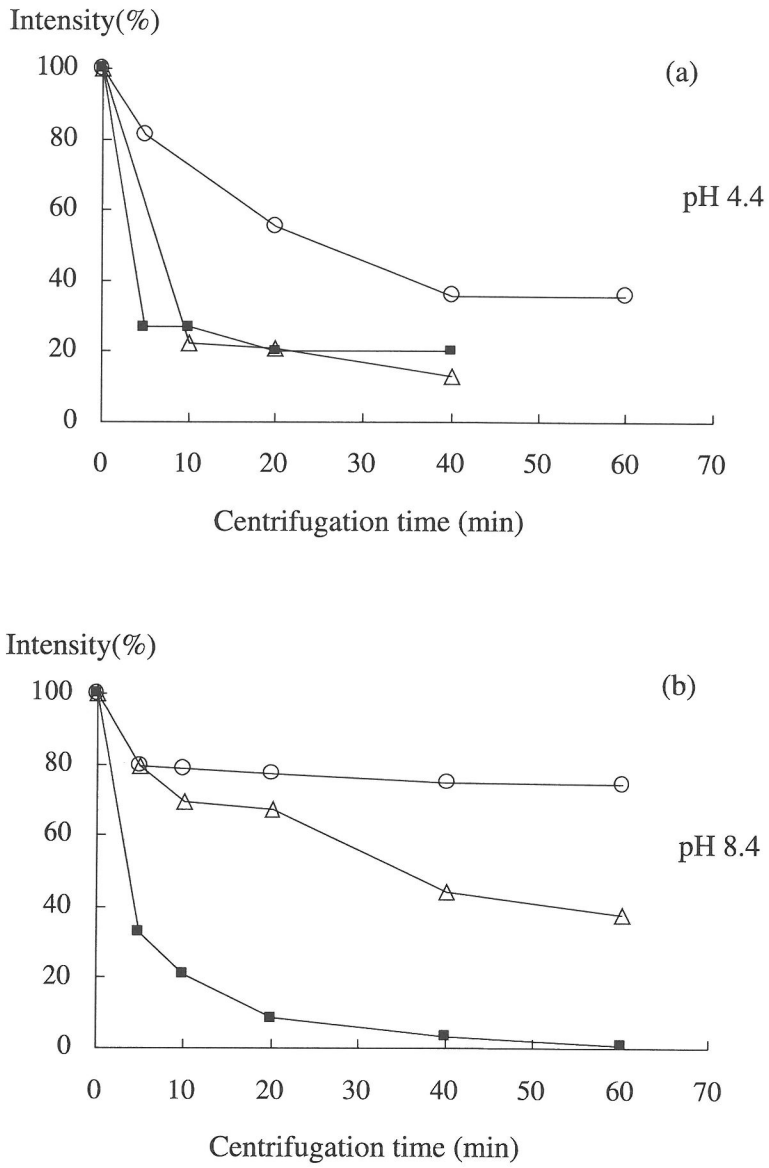

Fig. 8. Reduction of the observed fluorescence intensity (at 50.2 μs after the laser shot) after 5 to 60 minutes centrifugation at 1,000 (circles), 2,000 (triangles), and 10,000 (squares) rpm at pH 4.4 (a) and pH 8.4 (b).

attached to the quartz cell walls, may play a role in influencing the results.

In general, aggregation does occur where expected; the most rapid aggregation is observed in the slightly acidic pH range where silica particles have nearly no net surface charge. At acid pH, the proposed uranyl surface complex is also not charged. Intermediate aggregation is observed at pH 8.4 where silica particles have large negative surface charges and the proposed uranyl surface complex is also charged negatively. The 17 % uranyl at pH 4.4 which does not aggregate at all under the centrifugation conditions presented here is most probably bound to silicic acid, resulting in charged molecules (see Eqn. 8 in Table 2).

These results suggest that the risk of uranyl transfer by silica colloids in groundwater and the hydro-

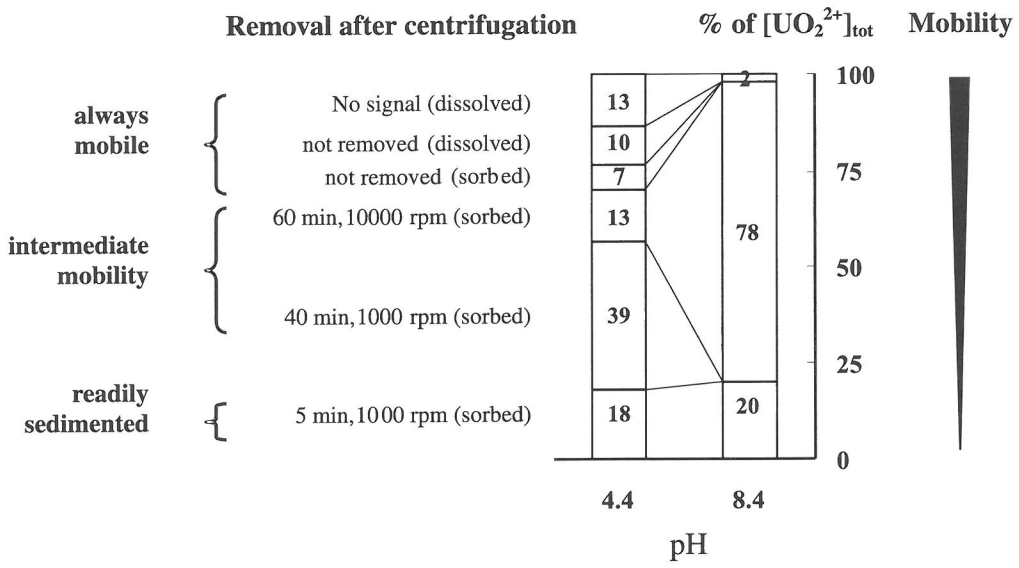

Fig. 9. Removed percentage of uranyl (% of total concentration) at different centrifugation conditions.

sphere is controlled not only by pH conditions, but also by the flow velocity. In slightly acidic waters, uranyl is more mobile as it may be complexed with aqueous silicic acid, and in slightly basic conditions it is potentially transported as a sorbed species on small silica particles which have an intermediate susceptibility to aggregation behavior.

4. CONCLUSIONS

For the first time, to our knowledge, two distinctively different molecular environments of uranyl sorbed on amorphous silica have been observed and quantified by spectroscopic analysis. This has been done by TRLIFS at trace-level concentrations, i.e., at levels not accessible to conventional spectroscopic techniques such as NMR or EXAFS. This is important since trace-level concentrations are perhaps more relevant to natural environments, and in addition sorption mechanisms may change with the sorbate to sorbant ratio, i.e., the structure of the surface complexes may change as a function of surface concentration (Morris et al., 1994; Chrisholm-Brause et al., 1994).

In general, uranyl adsorption to amorphous silica is known to result in the formation of bidentate surface complexes, where two water molecules in the equatorial plane of the uranyl ion are replaced by silanol groups (Dent et al., 1992, Reich et al., 1998, Sylwester et al., 2000). The different observed molecular environments in this study are thought to represent different levels of hydrolysis. Polymerization of uranyl seems unlikely as U-U near-order was observed in this system only at elevated uranyl concentrations likely to cause surface precipitation. The addition of ions such as carbonate or silicic acid may also cause a change in the structure of the surface complex. Carbonate ions are most likely not an integral part of the fluorescent surface species since they are known to drastically reduce fluorescence lifetimes in aqueous environments. At this point it seems very unlikely that sorbed silicic acid molecules are distinguishable from structural units belonging to amorphous silica. Therefore this process was not considered in the speciation calculations in the present study.

The two complexes observed by TRLIFS were assigned to $\equiv SiO_2UO_2^{\circ}$ and $\equiv SiO_2UO_2OH^-$ species. In accordance with literature data, the existence of a non-fluorescent uranyl-silica-carbonate-hydroxo complex $\equiv SiO_2UO_2OHCO_3^{3-}$ was postulated in order to account for the difference between the sum of the concentrations of the fluorescent surface complexes and the experimentally determined total sorbed uranyl concentration (Waite et al., 1994).

In this study silica particles were shown to be a potential candidate for facilitating the transport of uranium in subsoils. The major risk appears to occur in the acidic pH range where dissolved silicic acid

and a fraction of the silica particles, despite their nearly neutral surface charge, are least likely to aggregate and thus be removed from solution. Thus, under favorable transport conditions, uranium sorbed to silica may migrate in the subsoil.

Acknowledgements—We are grateful to the radiochemistry department of the Forschungszentrum Rossendorf, Germany, where U.G. spent several weeks for the TRLIFS measurements. We thank Gerhardt Geipel, Axel Brachmann, Henry Moll, Vinzenz Brendler, and Thorsten Stumpf from this department, whose valuable assistance helped immensely in the writing of this manuscript. U.G. thanks the "Pole Européen" (UJF-Grenoble) for a doctoral scholarship. The authors would like to express their gratitude to the group working on porous silica at the Spectrometry Physics Laboratory, Grenoble, for providing material and assistance for the elaboration of the device that was used to quantify the uranyl solution concentrations. We thank W. Runde, G. Bidoglio, E. Giffaut and one anonymous reviewer for their constructive comments which led to the improvement of the manuscript. We also thank Roland Hellmann for assistance in the analyses of the aqueous silica, for comments on the manuscript, and improving the English.

Editorial handling: R. Hellmann

REFERENCES

Bargar J. R., Reitmeyer R., and Davis J. A. (1999) Spectroscopic confirmation of uranium(VI) carbonate adsorption complexes on hematite. *Environ. Sci. Technol.* **33**, 2481-2484.

Bargar J. R., Reitmeyer R., Lenhardt J. J., and Davis J. A. (2000) Characterization of U(VI)-carbonate ternary complexes on hematite: EXAFS and electrophoretic mobility measurements. *Geochim. Cosmochim. Acta* **64**, 2737-2749.

Belyak Yu. N., Glinka Yu. D., Krut A. V., Naumenko S. N., Ogenko V. M., and Chuiko A. A. (1993) IR spectroscopic study of the dynamics of thermal dehydration and dehydroxylation of extremely hydrated samples of dispersed silica. *J. Appl. Spectroscopy* **59**, 515-522.

Bernhard G., Geipel G., Brendler V., and Nitsche H. (1996) Speciation of uranium in seepage waters of a mine tailing pile studied by time-resolved laser-induced fluorescence spectroscopy (TRLFS). *Radiochim. Acta* **74**, 87-91.

Berthoud T., Decambox P., Kirsch B., Maichien P., and Moulin C. (1988) Direct uranium trace analysis in plutonium solutions by time-resolved laser-induced spectrofluorometry. *Anal. Chem.* **60**, 1296-1299.

Brady P. V. and Walther J. W. (1990) Kinetics of quartz dissolution at low temperatures. *Chem. Geol.* **82**, 253-264.

Brendler V., Geipel G., Bernhard G., and Nitsche H. (1996) Complexation in the system $UO_2^{2+}/PO_4^{3-}/OH^-$(aq): potentiometric and spectroscopic investigations at very low ionic strengths. *Radiochim. Acta* **74**, 75-80.

Brina R. and Miller A.G. (1992) Direct determination of trace levels of uranium by laser-induced kinetic phosphorimetry. *Anal. Chem.* **64**, 1413-1418.

Burneau A. and Gallas J.-P. (1998) Hydroxyl groups on silica surfaces - Vibrational spectroscopies. In *The Surface Properties of Silicas* (ed. A.P. Legrand). John Wiley & Sons, Chichester, 147-234.

Charlet L., Schindler P. W., Spadini L., Furrer G., and Zysset M. (1993) Cation adsorption on oxides and clays: The aluminium case. *Aq. Sci.* **55**, 291-303.

Chrisholm-Brause C., Conradson S. D., Buscher C. T., Eller P. G., and Morris D. E. (1994) Speciation of uranyl sorbed at multiple binding sites on montmorillonite. *Geochim. Cosmochim. Acta* **58**, 3625-3631.

Costa D., Fubini B., Giamello E., and Volante M. (1990) A novel type of active site at the surface of crystalline SiO_2 (alpha-quartz) and its possible impact on pathogenicity. *Can. J. Chem.* **69**, 1427-1434.

Davies C. W. (1962) *Ion Association*. Butterworth, Washington, D.C.

Deniau H., Decambox P., Mauchien P., and Moulin C. (1993) Time-resolved laser-induced spectrofluorometry of UO_2^{2+} in nitric acid solutions. Preliminary results for on-line uranium monitoring applications. *Radiochim. Acta* **61**, 23-28.

Dent A. J., Ramsay D. F., and Swanton S. W. (1992) An EXAFS Study of uranyl ion in solution and sorbed onto silica and montmorillonite clay colloids. *J. Colloid Interface Sci.* **150**, 45-60.

Dove P. M. and Crerar D. A. (1990) Kinetics of quartz dissolution in electrolyte solutions using a hydrothermal mixed flow reactor. *Geochim. Cosmochim. Acta*, **54**, 955-969.

Dove P. M. and Rimstidt J. D. (1994) Silica-water-interactions. In *Silica: Physical Behavior, Geochemistry and Materials Applications* (eds. P.J. Heaney, C.T. Prewitt, and G.V. Gibbs). Reviews in Mineralogy **29**, Mineralogical Society of America, Washington, D.C., pp. 259-308.

Duff M. C., Morris D. E., Hunter D. B., and Bertsch P. M. (2000) Spectroscopic characterization of uranium in evaporation basin sediments. *Geochim. Cosmochim. Acta* **64**, 1535-1550.

Eliet V. (1996) Applications des techniques de fluorescence pour l'étude de l'uranium dans des milieux homogènes et hétérogènes: Réactions d'hydrolyse et photoréduction sur le bioxyde de titane. Ph.D. thesis, Université de Paris Sud, France.

Eliet V., Bidoglio G., Omenetto N., Parma L., and Grenthe I. (1995) Characterization of hydroxide complexes of uranium(VI) by time-resolved fluorescence spectroscopy. *J. Chem. Soc. Faraday Trans.* **91**, 2275-2285.

Farges F., Ponader C. W., Calas G., and Brown G. E. Jr. (1992) Structural environments of incompatible elements in silicate glass/melt systems. *Geochim. Cosmochim. Acta*, **56**, 4205-4220.

Gabriel U. (1998) Transport réactif de l'uranyle: Mode de fixation sur la silice et la goethite; expériences en colonne et réacteur fermé; simulations. Ph.D. thesis, Université Joseph Fourier, Grenoble, France.

Gabriel U., Gaudet J.-P., Spadini L., and Charlet L. (1998) Reactive transport of uranyl in a goethite column: An experimental and modelling study. *Chem. Geol.* **151**, 107-128.

Gampp H., Maeder M., Meyer C. J., and Zuberbuehler A. D. (1987) Evolving factor analysis. *Comments Inorg. Chem.* **6**, 41-60.

Giamelo E., Fubini B., Volante M., and Costa D. (1990) Surface oxygen radicals originating via redox reactions during the mechanical activation of crystalline SiO_2 in hydrogen peroxide. *Colloids and Surfaces* **45**, 155-165.

Glinka Y. D. and Krak T. B. (1995) Luminescence spectra of

uranyl ions adsorbed on disperse SiO_2 surfaces. *Physical Review B* **52**, 14985-14995.

Grenthe I., Fuger J., Konings R. J. M., Lemire R. J., Muller A. B., Nguyen Trung C., and Wanner H. (1992) *Chemical Thermodynamics of Uranium*. North Holland, Amsterdam.

Hommel H., Legrand A. P., Doremieux C., and D'espinose de la Caillerie J.-B. (1998) Hydroxyl groups on silica surfaces - NMR spectroscopies. In *The Surface Properties of Silicas*. (ed. A.P. Legrand). John Wiley & Sons, Chichester, 235-284.

Hudson E. A., Terminello L. J., Viani B. E., Reich T., Bucher J. J., Shuh D. K., and Edelstein N. M. (1995) X-ray absorption studies of uranium sorption on mineral substrates. In *Applications of Synchrotron Radiation Techniques to Material Science II. Symposium* (eds. L.J. Terminello, N.D. Shinn, G.E. Ice, K.L. D'Amico, and D.L. Perry). Materials Research Society, pp. 235-240.

James R. O. and Healy T. W. (1972) Adsorption of hydrolyzable ions at the oxide-water interface. I. Co(II) adsorption on SiO_2 and TiO_2 as model systems. *J. Colloid Interface. Sci.* **40**, 42-52.

Kato Y., Meinrath G., Kimura T., and Yoshida Z. (1994) A study of U(VI) hydrolysis and carbonate complexation by time-resolved laser-induced fluorescence spectroscopy (TRLFS). *Radiochim. Acta* **64**, 107-111.

Kushnirenko I. Ya., Glinka Yu. D., Degoda V. Ya., Krak T. B., and Ogenko V. M. (1993) Luminescent properties of uranyl ions adsorbed on the surface of disperse silicon dioxide. *J. Appl. Spectroscopy* **59**, 687-692.

Ludwig C. (1993) Koordinationschemie an der Grenzschicht Oxid/Wasser, I. Ternaere Oberflaechenkomplexe mit Cu(II) und organischen Liganden und TiO_2 (Anatas), II. Ein Modell zur Beschreibung der Deprotonierung von $Al_{13}O_4(OH)_{24}(H_2O)_{12}^{7+}$. Ph.D. thesis, University of Bern, Switzerland.

Meinrath G., Kato Y., and Yoshida Z. (1993) Spectroscopic Study of the uranyl hydrolysis species $(UO_2)_2(OH)_2^{2+}$. *J. Radioanal. Nucl. Chem.* **174**, 299-314.

Michard P., Guibal E., Vincent T., and Le Cloirec P. (1996) Sorption and desorption of uranyl ions by silica gel: pH, particle size, and porosity effects. *Microp. Mat.* **5**, 309-324.

Moll, H. (1997) Zur Wechselwirkung von Uran mit Silikat in waessrigen Systemen. Ph.D. thesis, TU Dresden, Germany.

Moll H., Geipel G., Matz W., Bernhard G., and Nitsche H. (1996) Solubility and speciation of $(UO_2)_2SiO_4 \cdot 2H_2O$ in aqueous systems. *Radiochim. Acta* **74**, 3-7.

Moll H., Geipel G., Brendler V., Bernhard G., and Nitsche H. (1998) Interaction of uranium(VI) with silicic acid in aqueous solutions by time-resolved laser-induced fluorescence spectroscopy (TRLFS). *J. Alloys & Compounds* **271-273**, 765-768.

Morris D. E., Chrisholm-Brause C. J., Barr M. E., Conradson S. D., and Eller P. G. (1994) Optical spectroscopic studies of the sorption of UO_2^{2+} species on a reference smectite. *Geochim. Cosmochim. Acta* **58**, 3613-3623.

Moulin C., Decambox P., Moulin V., and Decaillon J. G. (1995) Uranium speciation in solution by time-resolved laser-induced fluorescence. *Anal. Chem.* **67**, 348-353.

Östhols E. (1995) Thorium sorption on amorphous silica. *Geochim. Cosmochim. Acta* **59**, 1235-1249.

Pauling L. (1929) The principles determining the structure of complex ionic crystals. *J. Am. Chem. Soc.* **51**, 1010-1026.

Press W. H., Vetterling W. T., Teukolsky S. A., and Flammery B. A. (1992) *Numerical Recipes*, 2nd ed. Cambridge University Press, Cambridge.

Reich T., Moll H., Denecke M. A., Geipel G., Bernhard G., Nitsche H., Allen P. G., Bucher J.J., Kaltsoyannis N., Edelstein N. M., and Shuh D. K. (1996) Characterization of hydrous uranyl silicate by EXAFS. *Radiochim. Acta* **74**, 219-223.

Reich T., Moll H., Arnold T., Denecke M.A., Henning C., Geipel G., Bernhard G., Nitsche H., Allen P.G., Bucher J.J., Edelstein N.M., and Shuh D.K. (1998) An EXAFS study of uranium(VI) sorption onto silica gel and ferrihydrite. *J. Spectroscop. Related Phenom.* **96**, 237-243.

Schindler P. W. (1991) A solution chemist's view of surface chemistry. *Pure and Appl. Chem.* **63**, 1697-1704.

Schindler P. W. and Gamsjäger H. (1972) Acid-base reactions of the titanium dioxide (anatase)-water interface and the point of zero charge of titanium dioxide suspensions. *Kolloid -Z. u. Z. Polymere* **250**, 759-763.

Schindler P. W., Fuerst B., Dick R., and Wolf P. U. (1976) Ligand properties of surface silanol groups. I. Surface complex formation with iron(3+), copper(2+), cadmium(2+) and lead(2+). *J. Colloid. Interface Sci.* **55**, 469-475.

Stanton J. and Maatman R. W. (1963) The reaction between aqueous uranyl ion and the surface of silica gel. *J. Colloid Sci.* **18**, 132-146.

Strickland C. and Parsons J. L. (1972) Determination of reactive silicate. In *Practical Book of Sea Water Analysis*. Fisheries Research Board of Canada, pp. 65-70.

Stumm W. and Morgan J. J. (1996) *Aquatic Chemistry. Chemical Equilibria and Rates in Natural Waters*. John Wiley & Sons, Inc., New York.

Sylwester E. R., Hudson E. A., and Allen P. G. (2000) The structure of uranium(VI) sorption complexes on silica, alumina, and montmorillonite. *Geochim. Cosmochim. Acta* **64**, 2431-2438.

Van Cappellen P. and Gaillard J. F. (1996) Biogeochemical dynamics in aquatic sediments. In *Reactive Transport in Porous Media* (eds. P.C. Lichtner, C.I. Steefel, and E.H. Oelkers). Reviews in Mineralogy **34**, Mineralogical Society of America, Washington, D.C., pp. 335-376.

Van Cappellen P. and Qui L. (1997) Biogenic silica dissolution in sediments of the Southern Ocean. I. Solubility. *Deep-Sea Res. II* **44**, 1129-1149.

Waite T. D., Davis J. A., Payne T. E., Waychunas G. A., and Xu N. (1994) Uranium(VI) adsorption to ferrihydrite: Application of a surface complexation model. *Geochim. Cosmochim. Acta* **58**, 5465-5478.

Westall J. C. (1982) A computer program for the determination of chemical equilibrium constants from experimental data. Version 1.2. Oregon State University, Corvallis, Oregon, USA.

Wheeler J. and Thomas J. K. (1984) Photochemistry of the uranyl ion in colloidal silica solution. *J. Phys. Chem.* **88**, 750-754.